Opposite effect of membrane raft perturbation on transport activity of KCC2 and NKCC1

Anna-Maria Hartmann[1], Peter Blaesse[2], Thorsten Kranz[3,4], Meike Wenz[3], Jens Schindler[1], Kai Kaila[2], Eckhard Friauf[3], and Hans Gerd Nothwang[1,3*]

[1]Department of Neurogenetics, Institute for Biology and Environmental Sciences, Carl von Ossietzky University, Carl von Ossietzky Straße. 9-11, 26111 Oldenburg, Germany

[2]Department of Biosciences, University of Helsinki, Viikinkaari 1, 00014 Helsinki, Finland

[3]Animal Physiology Group, Department of Biology, University of Kaiserslautern, Erwin-Schrödinger Straße 13, 67663 Kaiserslautern, Germany

[4]present address: Psychobiology, Department of Behavioral Genetics, University of Trier, Johanniterufer 15, 54290 Trier, Germany

*Contact address:

Hans Gerd Nothwang

Department of Neurogenetics

Carl von Ossietzky University of Oldenburg

D-26111 Oldenburg

tel.: +49 -441-798-3932

fax.: +49 -441-798-3250

e-mail: hans.g.nothwang@uni-oldenburg.de

ABSTRACT

In the majority of neurons, the intracellular Cl^- concentration is set by the activity of the Na^+-K^+-$2Cl^-$ cotransporter NKCC1 and the K^+-Cl^- cotransporter KCC2. Here, we investigated the cotransporters' functional dependence on membrane rafts. In the mature rat brain, NKCC1 was mainly insoluble in Brij 58 and codistributed with the membrane raft marker flotillin-1 in sucrose density flotation experiments. In contrast, KCC2 was found in the insoluble fraction as well as in

the soluble fraction, where it codistributed with the non-raft marker transferrin receptor. Both KCC2 populations displayed a mature glycosylation pattern. Disrupting membrane rafts with methyl-β-cyclodextrin (MβCD) increased the solubility of KCC2, yet had no effect on NKCC1. In HEK-293 cells, KCC2 was strongly activated by a combined treatment with MβCD and sphingomyelinase, while NKCC1 was inhibited. These data indicate that membrane rafts render KCC2 inactive and NKCC1 active. In agreement with this, inactive KCC2 of the perinatal rat brainstem largely partitioned into membrane rafts. In addition, the exposure of the transporters to MβCD and sphingomyelinase showed that the two transporters differentially interact with membrane rafts. Taken together, membrane raft association appears to represent a mechanism for coordinated regulation of chloride transporter function.
Running Title: Role of membrane rafts in KCC2 and NKCC1 activity

INTRODUCTION

The intracellular Cl^- concentration ($[Cl^-]_i$) in neurons is mainly set by an interplay of the two cation chloride cotransporters NKCC1 and KCC2 (Blaesse *et al.* 2009;Delpire 2000). These proteins belong to the family of cation chloride cotransporters (CCC; Gamba 2005). In many immature neurons, NKCC1 provides the high $[Cl^-]_i$ required for the depolarizing action of GABA by a coupled Na^+-K^+-$2Cl^-$ import (Sipila *et al.* 2009;Achilles *et al.* 2007;Yamada *et al.* 2004). In contrast, KCC2 mediates the coupled export of K^+ and Cl^-, thereby generating an inwardly directed, hyperpolarizing electrochemical gradient for Cl^- in most adult neurons (Balakrishnan *et al.* 2003;Huebner *et al.* 2001;Rivera *et al.* 1999;Zhu *et al.* 2005).

KCC2 and NKCC1 are coexpressed in many neurons (Balakrishnan *et al.* 2003;Price and Trussell 2006;Vardi *et al.* 2000). Developmental immunoblot analysis demonstrated KCC2 in the immature brain (Blaesse *et al.* 2006), which also expresses high levels of NKCC1 (Plotkin *et al.* 1997). Mature cortical neurons express not only KCC2, but also NKCC1 to maintain a high $[Cl^-]_i$ in the axon initial segment (Khirug *et al.* 2008). This coexpression of a Cl^- uptake (NKCC1) and a Cl^- extrusion system (KCC2) requires a coordinated regulation of the two transporters. Previous studies have reported an opposite regulation of their transport activity via phosphorylation (Darman *et al.* 2001;de Los *et al.* 2006;Gagnon *et al.* 2006;Song *et al.* 2002) or via interaction with CIP1 (Caron *et al.* 2000;Wenz *et al.* 2009). However, the cellular mechanisms underlying transporter regulation are largely unknown.

In recent years, membrane rafts have been established as a cellular platform for the regulation of protein activity (Allen *et al.* 2007). Membrane rafts are small (10-200 nm diameter), highly dynamic, cholesterol-, sterol- and sphingolipid-enriched microdomains (Pike 2006). They have been associated with diverse functions, such as intracellular sorting of proteins, membrane trafficking, and signal transduction (Mishra and Joshi 2007). Proteins in membrane rafts resist cold extraction by non-ionic detergents and thereby display a low-buoyant density in sucrose flotation experiments. In contrast, detergent extraction disrupts lipid-protein interactions in non-raft domains, such that these proteins become solubilized and end up in the high-density fractions. In neurons, membrane rafts play an important role in neurotransmission and harbor acetylcholine receptors, glutamate receptors, $GABA_A$ receptors, as well as the transporters EAAT2, SERT, and NHE3 (Allen *et al.* 2007).

Recently, the CCC family members NCC and NKCC2 (Welker *et al.*, 2008) as well as KCC3 and KCC4 (Fujii *et al.*, 2008) were identified as membrane rafts-associated proteins. Here,

we addressed the question whether KCC2 and NKCC1 are localized to these membrane microdomains. For that purpose, we investigated the role of such rafts in KCC2 and NKCC1 transport activity.

MATERIALS AND METHODS

Animals were bred and housed in our animal facility and treated in compliance with the current Animal Protection Law. All protocols were approved by the regional animal care and use committees and adhered to the NIH Guide for the Care and Use of Laboratory Animals.

Membrane preparation from rat brain tissue

Rats were killed by decapitation during chloral hydrate-induced anesthesia (7 mg kg^{-1} body weight i.p.). Brains were rapidly dissected and stored at -80°C. Membrane fractions were isolated according to a previously published protocol (Guillemin *et al.* 2005) and either immediately subjected to detergent treatment or stored in aliquots at -80°C.

Isolation of membrane rafts

Membrane homogenates from brain tissue were treated in 3 ml TNE (50 mM Tris, 150 mM NaCl, 5 mM EDTA, pH 7,4) with 1% Brij 58 for 30 min on ice. The homogenate was then mixed with 2 ml 70% (w/v) sucrose solution in TNE, transferred into a polyallomer centrifuge tube (14 mm x 95 mm, Beckman Coulter, Krefeld, Germany), then carefully overlaid with 3.5 ml of 30% (w/v) sucrose solution in TNE and finally with 3.5 ml 5% (w/v) sucrose solution in TNE. Thereafter, discontinuous sucrose density gradient centrifugation was carried out at 4 °C for 22 h at 230,000×g, using a SW40 rotor and an Optima L-80 XP ultracentrifuge (Beckman Coulter). Twelve fractions of equal volume were collected from the bottom to the top of the discontinuous sucrose gradient.

Immunoblot analysis

Immunoblot analysis was conducted as described previously (Nothwang *et al.* 2003). Primary antibodies were anti-flotillin-1 (BD Biosciences, Heidelberg, Germany, dilution 1:500), anti-cKCC2 Blaesse et al., 2006, dilution 1:5,000), anti-NKCC1 (T4 antibody (Developmental Studies Hybridoma Bank Iowa, dilution 1:1,000), anti-Na$^+$/K$^+$-ATPase alpha subunit (a5, Developmental Studies Hybridoma Bank Iowa, dilution 1:1,000) and anti-transferrin receptor (Invitrogen, Karlsruhe, dilution 1:1,000). The secondary antibodies were goat anti-rabbit IgG or anti-mouse IgG horseradish peroxidase-conjugated (1:5,000, GE Healthcare, Freiburg, Germany). Bound

antibodies were detected using an enhanced chemiluminescence assay (Perkin Elmer) and a Las-3000 documentation system (Fuji).

Manipulation of membrane rafts

Cholesterol from brain membrane homogenates was depleted by four rounds of treatment with 50 mg/ml methyl-β-cyclodextrin (MβCD; Sigma, Taufkirchen, Germany) in 1 ml TNE on ice for 30 min. Solubilized cholesterol was removed by pelleting the membrane suspension at 100,000 x g for 30 min. Thererafter, membranes were treated with 1% Brij 58% at a protein to detergent ratio of 1 : 2.5. For cholesterol depletion of HEK-293 cells, cells were washed once with PBS and then incubated in 10 mg/ml MβCD in serum-free DMEM for 30 min at 37 °C. For treatment with sphingomyelinase (SMase, Sigma), cells were washed and incubated with 100 mU/ml for 1 hour 50 min at 37°C. When combining both treatments, cells were incubated at 37 °C first for 80 min with SMase, and then MβCD was added for 30 min. After treatment, cells were immediately processed for flux measurements, confocal imaging, cholesterol content, or cell viability measurements.

Cholesterol content of membranes was determined enzymatically using the Randox Cholesterol reagent kit in comparison with a cholesterol standard (Randox, Krefeld, Germany). Cell viability was tested in 96 well plates using the cytotoxicity assay MTT (3-[4,5-dimethylthiazol-2-yl]-2,5-diphenyl tetrazolium bromide) as previously described (Mosmann 1983). After cell treatment with SMase and MßCD, cells were washed twice with PBS and then incubated with 110 µl DMEM plus 5 mg/ml MTT reagent per well. After incubation for 4 h, solubilisation solution (10 % SDS in 0.01 mol/l HCl) was added and the plates were incubated over night at 37°C. The spectrophotometric absorbance of the purple formazan crystals were measured at 595 nm using an ELISA reader (Multiscan Ascent, Lab Systems, Vienna, USA). The reference wavelength was set to 800 nm.

Deglycosylation with EndoH or PGNase F

Deglycosylation experiments were performed using the endoglycosidase H (EndoH) or the *N*-glycosidase F (PGNase F) (New England Biolabs, Frankfurt, Germany). 25 µg of membrane proteins were first incubated for 10 min at 40 °C in glycoprotein denaturing buffer (0.5% SDS, 40 mM DTT) and then incubated for 2 h at 37 °C in either 50 mM sodium citrate (pH 5.5) at 37 °C, supplemented with 1,250 units EndoH, or in 50 mM sodium phosphate (pH 7.5), 1% NP-40, supplemented with 1,250 units PGNase. After incubation, samples were separated on a 4-12% Bis-Tris NuPAGE system for 2.5 h at 150 V.

Generation of expression constructs

Standard PCR and cloning techniques were used to generate KCC2 and NKCC1 expression constructs. The open reading frame (ORF) of rat KCC2 was cloned into the mammalian expression vector pEF5/FRT/V5-Dest (Invitrogen) and into the pEGFP-N3 vector (Clontech). The ORF of rat NKCC1 was cloned into the pDONR/Zeo vector (Invitrogen) and then moved into a Gateway-compatible pEGFP-N3 vector. All three constructs, KCC2-EF5/FRT/V5, KCC2-EGFP-N3, and NKCC1-EGFP-N 3 were used to generate HEK-293 cell lines stably expressing the transporters. To do so, cells transfected with the different constructs were selected for stable integration by culturing them in the presence of 1.5 mg/ml hygromycin or G418 (Invitrogen).

Determination of transport activity

Transport activity was assessed in HEK-293 cells by measuring Cl^--dependent uptake of $^{86}Rb^+$ (PerkinElmer Life Sciences, Rodgau-Juegesheim, Germany), a congener of K^+. HEK-293 cells were grown to 100% confluency on poly-L-lysine-coated wells of a 6 well culture dish. To determine KCC2 transport activity, cells were incubated in 1 ml preincubation buffer (100 mM N-methyl-D-glucamine-chloride, 5 mM KCl, 2 mM $CaCl_2$, 0.8 mM $MgSO_4$, 5 mM glucose, 5 mM HEPES, pH 7.4, 0.1 mM oubain). After 30 min at 37°C, the preincubation buffer was replaced by 1 ml incubation buffer (preincubation buffer containing 37 MBq $^{86}Rb^+$) incubated for another 7 min at room temperature. Following three washing steps in 1 ml ice-cold preincubation buffer without oubain, cells were lysed in 500 µl 0.25 M NaOH for 1 h. $^{86}Rb^+$ uptake was assayed by the determination of Cerenkov radiation and the protein amount was determined by the BCA Assay (Pierce). Flux data were corrected for changes in cell viability by subtracting the protein amount corresponding to dead cells from the total protein amount determined after flux measurements.

NKCC1 transport activity was determined using a modified protocol of (Dehaye *et al.* 2003). Cells were washed twice with preincubation buffer (135 mM NaCl; 2.5 mM KCl; 1 mM $CaCl_2$; 1 mM MgCl2; 15 mM Na-HEPES; 5 mM glucose; pH 7.4) and then incubated for 10 min at 37 °C. The wells were washed with hypertonic chloride-free media (135 mM; Na-gluconate; 2.5 mM K-gluconate; 1 mM $CaCl_2$; 1 mM $MgCl_2$; 15 mM HEPES; 5 mM glucose; 100 mM sucrose; pH 7.4) before they were incubated for 1 h at 37 °C. The chloride-free media was then replaced by chloride-free media plus 0.1 mM ouabain for further 10 min at 37 °C. Therafter, $^{86}Rb^+$ uptake was measured in uptake media (135 mM NaCl; 1mM KCl; 1 mM $CaCl_2$; 15 mM Na-HEPES; 5 mM glucose; 0.1 mM ouabain; 0.3 µCi $^{86}Rb^+$; pH 7.4) for 7 min at room

temperature. Following three washing steps in 1 ml ice-cold termination media (135 mM Na-gluconate; 7.5 mM NaCl; 15 mM HEPES; pH 7.4), cells were lysed in 500 µl 0.25 M NaOH for 1 h. At least 6 replicas were performed for each experiment. Data are given as mean ± s.d. Significant differences between the groups were analyzed by student`s *t* test.

Confocal imaging

To visualize the distribution of the KCC2- and NKCC1-EGFP fusion proteins after membrane raft perturbation, HEK-293 cells cultured on sterile glass coverslips pre-treated with 0.1 mg/ml poly-L-lysine were washed once with PBS and fixed with 4% paraformaldehyde in 0.2 M phosphate buffer for 15 min at room temperature. After fixation, cells were washed three times with PBS and mounted onto glass slides with Vectorshield Hard Set mounting medium (Vector laboratories, Burlingame, CA). Photomicrographs were taken using a SP5 confocal microscope (Leica, Wetzlar, Germany) equipped with a 63×1.3 NA glycerol immersion objective. The pinhole diameter was set for 1 Airy Unit.

RESULTS

Association of KCC2 and NKCC1 with membrane rafts in the mature brain

In order to investigate whether KCC2 and NKCC1 are associated with membrane rafts, these membrane domains were isolated from P25-30 rat brains by flotation experiments (Pike 2006). We extracted the membranes using 1% Brij 58 at a protein to detergent ratio of 1:2.5 and separated detergent-soluble from detergent-insoluble proteins by discontinuous sucrose gradient centrifugation. Collected fractions were assessed by immunoblot analysis for the presence of KCC2 and NKCC1, as well as for the membrane raft marker protein flotillin-1 (Bickel *et al.* 1997) and the transferrin receptor (TfR), a non-raft marker protein (Harder *et al.* 1998) (Fig. 1). The separation of flotillin-1 from TfR demonstrated the successful separation of membrane rafts from non-raft domains (Fig. 1A). We detected two KCC2 populations after Brij 58 treatment. One part of KCC2 was recovered in the low-density fractions 4-6 and codistributed with flotillin-1. A second population codistributed with TfR predominantly in the high-density fractions 10-12 (Fig. 1A). The immunoblot analysis showed similar amounts of KCC2 in both populations (Fig. 1A). The higher molecular weight of KCC2 mainly observed in the high-density fractions 10-12 compared to insoluble KCC2 in the lower-density fractions was likely due to aggregation of the protein in the absence of a lipid environment during centrifugation, as treatment with high

concentrations of reducing agents prior to gel electrophoresis did not result in any mobility shift (data not shown). It was therefore not possible to judge whether the Brij 58 soluble KCC2 population represented oligomeric KCC2 and the Brij 58 insoluble population monomeric KCC2 (Blaesse et al., 2006). Unlike KCC2, most NKCC1 was detected in the lower-density fractions 4-6, together with flotillin-1 (Fig. 1A). As the protein to detergent ratio is a key parameter with great influence on the outcome in flotation experiments (Allen *et al.* 2007;Scandroglio *et al.* 2008), we varied this ratio from 1:1 to 1:10. This only slightly affected solubilization of KCC2 and NKCC1 in Brij 58 (data not shown).

The data obtained so far implied that KCC2 is localized both to membrane rafts and non-raft domains, whereas NKCC1 is mainly associated with Brij 58-resistant membrane rafts. As cholesterol is a major component of membrane rafts, we assessed whether perturbing the membrane cholesterol content resulted in increased solubility of the membrane raft-associated transporters. One means to disrupt the organization of cholesterol-rich microdomains is cholesterol depletion by methyl-β-cyclodextrin (MβCD) (Butchbach *et al.* 2004;Magnani *et al.* 2004;Schuck *et al.* 2003;Taverna *et al.* 2004). We therefore incubated membrane homogenates with MβCD prior to Brij 58 treatment. A 60% reduction of cholesterol did not alter the distribution of KCC2, and a 70% reduction partially shifted KCC2 from the lower-density fractions to higher-density fractions (data not shown). An almost complete depletion of cholesterol resulted in a strong increase in solubilized KCC2, as most immunoreactivity was recovered in fractions 8-12 (Fig. 1B) and thus shifted by four fractions compared to Brij 58 treatment without previous cholesterol depletion. By contrast, NKCC1 was still recovered in lower-density fractions. This observation was reminiscent of the minor shift of the membrane raft-associated NKCC2 after MβCD treatment of cultured renal tubular cells (Welker *et al*., 2008). We therefore concluded that NKCC1 is associated with membrane rafts, whereas KCC2 forms two populations, with one being located outside rafts.

Finally, we analyzed the distribution of the Na^+/K^+-ATPase, whose association with transport-active KCC2 has been suggested (Ikeda *et al.* 2004). The large majority of this protein became solubilized in Brij 58 and was recovered in fractions 9-12 (Fig. 1A). After MβCD treatment, all Na^+/K^+-ATPase was observed in fractions 8-12 (Fig. 1B). This finding conforms to previous studies reporting the Na^+/K^+-ATPase as a non-membrane raft protein (Eckert *et al.* 2003;Nini *et al.* 2007;Becher *et al.* 2001).

Glycosylation pattern of raft-associated and non-raft-associated cotransporters

One explanation for the two KCC2 populations that we found is a different localization within specific subcellular compartments. The membrane preparation used for our flotation experiments represents a mixture of the plasma membrane and membranes of intracellular compartments such as the endoplasmic reticulum and the Golgi apparatus. To check whether one population represents intracellular KCC2, we enzymatically deglycosylated the two KCC2 populations obtained by Brij 58 treatment. The endoglycosidase EndoH cleaves mainly high-mannose glycosylated forms, which are indicative of proteins within the endoplasmic reticulum (Maley *et al.* 1989). The amidase PGNase F cleaves also complex oligosaccharides from *N*-linked glycoproteins, which form during the passage through the Golgi apparatus (Maley *et al.* 1989). We performed the deglycosylation experiments on pooled fractions 4-6 and 10-12. After incubation with the respective enzyme, proteins were analyzed by immunoblotting. Both KCC2 populations were insensitive to EndoH (Fig. 2A). In contrast, PGNase F treatment resulted in a shift of both KCC2 populations towards lower molecular weights compared to untreated samples (Fig. 2B). The increased molecular weight of KCC2 in the Brij 58-insoluble pool, compared to the untreated fractions (cf. Fig. 1A), probably reflects an aggregation of the transporter caused by the required denaturing protocol prior to enzymatic treatment. The data demonstrate that both the soluble and the insoluble KCC2 population display a mature glycosylation pattern and likely represent KCC2 from compartments distal to the cis-Golgi, and likely from plasma membrane.

Influence of membrane raft perturbation on KCC2 and NKCC1 transport activity

To further investigate the role of membrane rafts in KCC2 and NKCC1 function, we studied the effects of cholesterol depletion on $^{86}Rb^+$ transport (Williams and Payne 2004;Gagnon *et al.* 2006;Mercado *et al.* 2006). To examine the influence of membrane rafts on the functionality of KCC2, we used a HEK-293 cell line which stably expresses this transporter (HEK-293^{KCC2}). NKCC1 is endogenously expressed in HEK-293 cells (Isenring *et al.* 1998;Dehaye *et al.* 2003;Delpire *et al.* 2009). Our previous flotation experiments indicated a strong association of NKCC1 with membrane rafts. We therefore used three different protocols to disrupt membrane rafts. Cell cultures were treated either with 10 mg/ml MβCD for 30 min (Magnani *et al.* 2004), or with 100 mU/ml sphingomyelinase (SMase) (Scheek *et al.* 1997;Fischer *et al.* 2007), or with a combination of both agents. SMase hydrolyses the membrane raft component sphingomyelin to ceramide (Yu *et al.* 2005). First, we analyzed the effect of the treatments on the effectiveness of the cholesterol depletion and cell viability (suppl. Fig. 1). 45% of cholesterol was sequestered by the MβCD treatment (suppl. Fig. 1A). This was similar to a previously reported depletion of

~50% in HEK-293 cells (Magnani *et al.* 2004). The remaining cholesterol likely reflects the fact that MβCD is membrane-impermeable and does therefore not deplete cholesterol from intracellular membranes. Cell viability was 88% after MβCD treatment, 92% after SMase treatment, and 74% after combined treatment (Fig. 3B). Single treatment thus barely affected viability, and the viability was still high after combined treatment.

Next, we determined the flux activity after perturbation experiments. To do so, we first confirmed pharmacologically the presence of KCC2- and NKCC1-mediated fluxes in the cell lines used for this study. The ^{86}Rb influx was 1.8 fold higher in HEK-293^{KCC2} cells than in native HEK-293 cells (14.4 ± 2.4 nmoles × mg protein^{-1} × min^{-1} vs 7.99 ± 2.0 nmoles × mg protein^{-1} × min^{-1}). This increase was highly significant (p = 7.4 x 10^{-7}) and the flux was reduced by 45% in the presence of 2 mM furosemide, similar to a previous study (Strange *et al.* 2000). Native HEK-293 cells displayed Rb$^+$ uptake, which was blocked by 10 µM bumetanide (Fig, 3B; remaining activity: 2.3%), a concentration that is relatively specific for NKCCs (Blaesse *et al.* 2009;Russell 2000). The activity of KCC2 increased 3-fold after MβCD treatment (Fig, 3A; 300.1 ± 45.7%; p = 8.4×10^{-19}). The combined MβCD and SMase treatment resulted in an increased KCC2 activity of 671.7 ± 152.4% of the control (p = 6.9×10^{-20}) (Fig. 3A). SMase alone activated KCC2 only to a small, albeit significant extent (142.9 ± 15.1%; p = 6.1×10^{-12}) (Fig. 3A). The observed increase after all treatments was blocked by furosemide (Fig. 3A) and was always significantly different from those observed in native HEK-293 cells subjected to the same treatment (data not shown). Unlike KCC2, NKCC1 transport activity after cholesterol depletion by MβCD (144 ± 19.1%, p = 1.1×10^{-6}) was only slightly increased compared to untreated cells (Fig. 3B). This increase was completely blocked by 10 µM bumetanide (Fig. 3B). In contrast, breaking down sphingomyelin by SMase reduced NKCC1 activity almost 2-fold (58.3 ± 9.6%; p = 1.3×10^{-7}) (Fig. 3B). Similar to KCC2, the combined action of both agents had a more pronounced effect than either treatment alone and reduced NKCC1 activity to 38.6 ± 17.1% (p = 2×10^{-9}) (Fig. 3B).

Effect of membrane raft disruption on KCC2 and NKCC1 localization

The observed changes in transport activity after disruption of membrane rafts prompted us to ask whether the location of the transporters was altered. To address this issue, we used HEK-293 cells which stably express KCC2-EGFP or NKCC1-EGFP fusion proteins; in both constructs, EGFP was fused to the intracellular C-terminus of the transporters. In untreated controls, we observed a granular staining pattern at the plasma membrane of the cells for both, KCC2 and NKCC1 (Fig.

4A, E, I, M). The first and third rows depict cross sections and the second and fourth rows the basal surface of the same cell. After treatment with MβCD, a slighty more pronounced staining at the plasma membrane was apparent for both transporters (Fig. 4B, F, J, N), which is consistent with the transport results (Fig. 3). SMase alone resulted in no visible changes in KCC2 and NKCC1 distribution (Fig. 4C, G, K, O). The combined MβCD and SMase treatment resulted in large, sharp clusters of the transporters at the plasma membrane (Fig. 4D, H, L, P). These data indicate that perturbation of membrane rafts affects the localization of the transporters at the plasma membrane.

KCC2 association with membrane rafts in the immature brainstem
Our data from the flux measurements in HEK-293 cells indicated that the detergent-insoluble KCC2 population, which we observed in flotation experiments of the mature brain, corresponds to transport-inactive KCC2, whereas the detergent-soluble population represents transport-active KCC2. We therefore analyzed KCC2 partitioning in the brainstem at P0-2. At this immature age, most KCC2 is thought to be transport-inactive (Blaesse *et al.* 2006). According to our conclusion from the flux measurements that the membrane raft-associated KCC2 population of the mature brain represents transport-inactive KCC2, we expected to recover KCC2 in the membrane raft fraction at P0-2. Indeed, after treatment with Brij 58, KCC2 ended up in the low-density fractions 3 and 4, together with the membrane raft marker protein flotillin-1 (Fig. 5A). Only a minor amount of KCC2 was solubilized. Similar to P25-30, we observed higher molecular weight KCC2 aggregates. They were distributed throughout the gradient mirroring the distribution of monomeric KCC2 at 130 kDa.

To assess whether the presence of KCC2 in membrane rafts in the immature brainstem was due to the segregation into cholesterol-rich membrane rafts, as observed in the mature brain, we depleted cholesterol with MβCD from the membrane homogenate. Under this condition, which extracted ~70% cholesterol from the membranes, most KCC2 was soluble in Brij 58 and consequently, it recovered at higher densities, mainly in fractions 6 and higher (Fig. 5B). This shift towards higher-density fractions was thus similar to the cholesterol depletion experiments in the mature brain (cf. Fig. 1B). Together, these data support the idea that partitioning into membrane rafts renders KCC2 inactive.

DISCUSSION

Interactions between proteins and lipids are essential to many cellular functions. The present work investigated the association of two essential cotransporters for neuronal Cl$^-$ homeostasis, KCC2 and NKCC1, with membrane rafts. Two main findings arose from our study. (i) Membrane raft perturbations have opposite effects on the activity of the two cotransporters. (ii) The two cotransporters differentially associate with membrane raft microdomains.

Modulation of KCC2 and NKCC1 transport activity by membrane rafts

A defining characteristic of membrane raft proteins is their resistance to solubilization in non-ionic detergents. By means of flotation experiments, about half of KCC2 and the majority of NKCC1 codistributed with the membrane raft marker flotillin-1 in the lower-density fractions. This provided strong evidence that a considerable portion of both cotransporters is associated with membrane rafts, similar to the CCC family members KCC3, KCC4 (Fujii *et al.* 2008), NKCC1, and NCC (Welker *et al.* 2008). We used Brij 58 instead of Triton X-100, as the former was previously shown to be better suited to analyze the membrane raft association of the neuronal transporters SERT (Magnani *et al.* 2004) and EAAT2 (Butchbach *et al.* 2004).

To determine the physiological relevance of this segregation into membrane rafts, we disrupted these domains in HEK-293 cells, which are a widely used mammalian expression system for these CCC transporters (Simard *et al.* 2004;Moore-Hoon and Turner 2000;Wenz *et al.* 2009). Furthermore, HEK-293 cells faithfully reproduce the differential targeting of neuronal potassium channels to distinct membrane rafts (O'Connell and Tamkun 2005). The pivotal result of these experiments was that KCC2 was activated by perturbation of membrane rafts, whereas NKCC1 was inhibited (Fig. 3). This modulation likely occurred via a change in the distribution of the transporters at the plasma membrane as evidenced by confocal imaging analysis (Fig. 4).

The functional dependence of NKCC1 on the integrity of membrane rafts, together with its location in these microdomains, identifies the cotransporter as a bona fide membrane raft protein. Unlike NKCC1, flotation experiments demonstrated two populations for KCC2 in the brain, a detergent-soluble and a detergent-resistant pool (Fig. 1). Both populations displayed a mature glycosylation pattern, indicating that they originated from compartments distal to the cis-Golgi, and likely from the plasma membrane (Fig. 2). The observed activation of KCC2 after cholesterol depletion suggests that the detergent-soluble population represents constitutively transport-active KCC2 in the plasma membrane of unperturbed cells. In contrast, transport-inactive KCC2 constitutes the insoluble population, which can be activated by perturbation

experiments. This is analogous to the two populations of the src-family tyrosine kinase LCK, where the membrane raft-associated enzyme displays low activity and the non-membrane raft population high activity (Kabouridis *et al.* 2000;Rodgers and Rose 1996). Our analysis of the immature brainstem, which contains mainly inactive KCC2 (Blaesse *et al.* 2006), is in agreement with this conclusion. At this developmental stage, KCC2 mainly partitioned into membrane rafts. This was evidenced by codistribution of KCC2 with the membrane raft marker flotillin-1 and its shift to higher-density fractions after cholesterol depletion with MβCD.

It is of note that in neuronal cells, the Na^+/K^+-ATPase is mainly observed in the non-membrane raft fraction (Eckert *et al.* 2003;Nini *et al.* 2007). This conforms with the observation that this primary active transporter interacts with KCC2 to form a larger complex, allowing for efficient functional coupling in the nervous system at the molecular level (Ikeda *et al.* 2004). The functional role of membrane rafts in KCC3 and KCC4 transport activity has not yet been investigated (Fujii *et al.* 2008). It is therefore unclear whether other KCC family members require membrane rafts for proper transport activity.

Due to the opposite effect of membrane rafts on the activity of KCC2 and NKCC1, a shared regulatory mechanism for localization to membrane rafts would allow for efficient and dynamic regulation of $[Cl^-]_i$ in neurons. It is currently unknown whether a shared mechanism exists and how dynamically the two transporters can shift between different membrane compartments. In many cases, proteins are targeted to membrane rafts either via protein-protein interaction or by protein modification, such as acylation. It might also be worthwhile to investigate whether the reciprocal effect of phosphorylation on the activity of the two transporters (Gagnon *et al.* 2006;Kahle *et al.* 2005) involves their redistribution between different plasma membrane compartments. It will also be important to study whether the location of transport-active KCC2 outside membrane rafts and of NKCC1 within membrane rafts participates in the different subcellular distribution of the two transporters, such as the axonal localization of NKCC1 (Khirug *et al.* 2008).

KCC2 and NKCC1 differentially associate with membrane rafts

We observed strikingly different sensitivities of the two cotransporters towards the two membrane raft disturbing agents MβCD and SMase (Fig. 3). Cholesterol depletion by MβCD activated KCC2, whereas it only slightly affected NKCC1 transport activity. In keeping with this finding, MβCD treatment of brain membranes shifted the distribution of KCC2, but not of NKCC1 (Fig. 1). However, it is of note that we had to deplete cholesterol by $\geq 70\%$ in the brain

before observing a visible increase in KCC2 solubility after Brij 58% treatment. This indicates a rather strong association of KCC2 with membrane rafts, as a 60% cholesterol depletion was already sufficient to shift, for instance, the $Ca_v2.1$ subunit (Taverna *et al.* 2004).

In contrast to cholesterol depletion, the break-down of sphingomyelin by SMase reduced NKCC1 activity by ~50%, whereas KCC2 was only slightly affected by this treatment (Fig. 3). Insensitivity to SMase has already been observed for other membrane raft proteins. A mass spectrometric analysis revealed only a selective loss of proteins from membrane rafts after SMase treatment (Yu *et al.* 2005). G-proteins and flotillins remained associated with membrane rafts under this condition, whereas their level in membrane rafts decreased after cholesterol depletion (Foster *et al.* 2003;Yu *et al.* 2005). Furthermore, no reduction in membrane raft association was observed for the proteins PLAP, YES, caveolin-1, and VIP17 (Schuck *et al.* 2003). We attempted to analyze the effect of SMase on the distribution of the two transporters by sucrose gradient centrifugation. However, treatment by SMase resulted in aggregated membrane fractions which prevented further flotation experiments (A.M.H. and H.G.N., unpublished data).

The underlying mechanism of this different sensitivity to membrane raft perturbing agents is currently unclear. It might be either caused by an association of KCC2 and NKCC1 with different components within the same membrane rafts or by localization into different membrane rafts. Recent data indicated a rather high degree of heterogeneity within membrane rafts (Pike 2004;Mishra and Joshi 2007). Immunofluorescent probes and immuncytochemical labeling of raft-specific lipids and proteins as well as biochemical analysis will help to distinguish between these two possibilities.

In conclusion, our data identify a cellular mechanism for the coordinated regulation of NKCC1 and KCC2 during neuronal development as well as in subcellular domains.

ACKNOWLEDGEMENTS

developed under the auspices of the NICHD and maintained by The University of Iowa, Department of Biological Sciences, Iowa City, IA 52242, USA.

Reference List

Achilles K., Okabe A., Ikeda M., Shimizu-Okabe C., Yamada J., Fukuda A., Luhmann H. J. and Kilb W. (2007) Kinetic properties of Cl uptake mediated by Na+-dependent K+-2Cl cotransport in immature rat neocortical neurons. *J. Neurosci.* **27,** 8616-8627.

Allen J. A., Halverson-Tamboli R. A. and Rasenick M. M. (2007) Lipid raft microdomains and neurotransmitter signalling. *Nat. Rev. Neurosci.* **8,** 128-140.

Balakrishnan V., Becker M., Loehrke S., Nothwang H. G., Guresir E. and Friauf E. (2003) Expression and function of chloride transporters during development of inhibitory neurotransmission in the auditory brainstem. *J. Neurosci.* **23,** 4134-4145.

Becher A., White J. H. and McIlhinney R. A. (2001) The gamma-aminobutyric acid receptor B, but not the metabotropic glutamate receptor type-1, associates with lipid rafts in the rat cerebellum. *J. Neurochem.* **79,** 787-795.

Bickel P. E., Scherer P. E., Schnitzer J. E., Oh P., Lisanti M. P. and Lodish H. F. (1997) Flotillin and epidermal surface antigen define a new family of caveolae-associated integral membrane proteins. *J. Biol. Chem.* **272,** 13793-13802.

Blaesse P., Airaksinen M. S., Rivera C. and Kaila K. (2009) Cation-chloride cotransporters and neuronal function. *Neuron* **61,** 820-838.

Blaesse P., Guillemin I., Schindler J., Schweizer M., Delpire E., Khiroug L., Friauf E. and Nothwang H. G. (2006) Oligomerization of KCC2 correlates with development of inhibitory neurotransmission. *J. Neurosci.* **26,** 10407-10419.

Butchbach M. E., Tian G., Guo H. and Lin C. L. (2004) Association of excitatory amino acid transporters, especially EAAT2, with cholesterol-rich lipid raft microdomains: importance for excitatory amino acid transporter localization and function. *J. Biol. Chem.* **279,** 34388-34396.

Caron L., Rousseau F., Gagnon E. and Isenring P. (2000) Cloning and functional characterization of a cation-Cl- cotransporter-interacting protein. *J. Biol. Chem.* **275,** 32027-32036.

Darman R. B., Flemmer A. and Forbush B. (2001) Modulation of ion transport by direct targeting of protein phosphatase type 1 to the Na-K-Cl cotransporter. *J. Biol. Chem.* **276,** 34359-34362.

de Los H. P., Kahle K. T., Rinehart J., Bobadilla N. A., Vazquez N., San Cristobal P., Mount D. B., Lifton R. P., Hebert S. C. and Gamba G. (2006) WNK3 bypasses the tonicity requirement for K-Cl cotransporter activation via a phosphatase-dependent pathway. *Proc. Natl. Acad. Sci. U. S. A* **103,** 1976-1981.

Dehaye J. P., Nagy A., Premkumar A. and Turner R. J. (2003) Identification of a functionally important conformation-sensitive region of the secretory Na+-K+-2Cl- cotransporter (NKCC1). *J. Biol. Chem.* **278,** 11811-11817.

Delpire E. (2000) Cation-chloride cotransporters in neuronal communication. *News Physiol. Sci.* **15,** 309-312.

Delpire E., Days E., Lewis L. M., Mi D., Kim K., Lindsley C. W. and Weaver C. D. (2009) Small-molecule screen identifies inhibitors of the neuronal K-Cl cotransporter KCC2. *Proc. Natl. Acad. Sci. U. S. A*. **106**, 5383-8.

Eckert G. P., Igbavboa U., Muller W. E. and Wood W. G. (2003) Lipid rafts of purified mouse brain synaptosomes prepared with or without detergent reveal different lipid and protein domains. *Brain Res.* **962,** 144-150.

Fischer H., Ellstrom P., Ekstrom K., Gustafsson L., Gustafsson M. and Svanborg C. (2007) Ceramide as a TLR4 agonist; a putative signalling intermediate between sphingolipid receptors for microbial ligands and TLR4. *Cell Microbiol.* **9,** 1239-1251.

Foster L. J., de Hoog C. L. and Mann M. (2003) Unbiased quantitative proteomics of lipid rafts reveals high specificity for signaling factors. *Proc. Natl. Acad. Sci. U. S. A* **100,** 5813-5818.

Fujii T., Takahashi Y., Itomi Y., Fujita K., Morii M., Tabuchi Y., Asano S., Tsukada K., Takeguchi N. and Sakai H. (2008) K+-Cl- Cotransporter-3a Up-regulates Na+,K+-ATPase in Lipid Rafts of Gastric Luminal Parietal Cells. *J. Biol. Chem.* **283,** 6869-6877.

Gagnon K. B., England R. and Delpire E. (2006) Volume sensitivity of cation-Cl- cotransporters is modulated by the interaction of two kinases: Ste20-related proline-alanine-rich kinase and WNK4. *Am. J. Physiol Cell Physiol* **290,** C134-C142.

Gamba G. (2005) Molecular physiology and pathophysiology of electroneutral cation-chloride cotransporters. *Physiol Rev.* **85,** 423-493.

Guillemin I., Becker M., Ociepka K., Friauf E. and Nothwang H. G. (2005) A subcellular prefractionation protocol for minute amounts of mammalian cell cultures and tissue. *Proteomics.* **5,** 35-45.

Harder T., Scheiffele P., Verkade P. and Simons K. (1998) Lipid domain structure of the plasma membrane revealed by patching of membrane components. *J. Cell Biol.* **141,** 929-942.

Huebner C. A., Stein V., Hermans-Borgmeyer I., Meyer T., Ballanyi K. and Jentsch T. J. (2001) Disruption of KCC2 reveals an essential role of K-Cl cotransport already in early synaptic inhibition. *Neuron* **30,** 515-524.

Ikeda K., Onimaru H., Yamada J., Inoue K., Ueno S., Onaka T., Toyoda H., Arata A., Ishikawa T. O., Taketo M. M., Fukuda A. and Kawakami K. (2004) Malfunction of respiratory-related neuronal activity in Na+, K+-ATPase alpha2 subunit-deficient mice is attributable to abnormal Cl- homeostasis in brainstem neurons. *J. Neurosci.* **24,** 10693-10701.

Isenring P., Jacoby S. C., Payne J. A. and Forbush B., III (1998) Comparison of Na-K-Cl cotransporters. NKCC1, NKCC2, and the HEK cell Na-L-Cl cotransporter. *J. Biol. Chem.* **273,** 11295-11301.

Kabouridis P. S., Janzen J., Magee A. L. and Ley S. C. (2000) Cholesterol depletion disrupts lipid rafts and modulates the activity of multiple signaling pathways in T lymphocytes. *Eur. J. Immunol.* **30,** 954-963.

Kahle K. T., Rinehart J., de Los H. P., Louvi A., Meade P., Vazquez N., Hebert S. C., Gamba G., Gimenez I. and Lifton R. P. (2005) WNK3 modulates transport of Cl- in and out of cells: Implications for control of cell volume and neuronal excitability. *Proc. Natl. Acad. Sci. U. S. A* **102,** 16783-16788.

Khirug S., Yamada J., Afzalov R., Voipio J., Khiroug L. and Kaila K. (2008) GABAergic depolarization of the axon initial segment in cortical principal neurons is caused by the Na-K-2Cl cotransporter NKCC1. *J. Neurosci.* **28,** 4635-4639.

Magnani F., Tate C. G., Wynne S., Williams C. and Haase J. (2004) Partitioning of the serotonin transporter into lipid microdomains modulates transport of serotonin. *J. Biol. Chem.* **279,** 38770-38778.

Maley F., Trimble R. B., Tarentino A. L. and Plummer T. H., Jr. (1989) Characterization of glycoproteins and their associated oligosaccharides through the use of endoglycosidases. *Anal. Biochem.* **180,** 195-204.

Mercado A., Broumand V., Zandi-Nejad K., Enck A. H. and Mount D. B. (2006) A C-terminal domain in KCC2 confers constitutive K+-Cl- cotransport. *J. Biol. Chem.* **281,** 1016-1026.

Mishra S. and Joshi P. G. (2007) Lipid raft heterogeneity: an enigma. *J. Neurochem.* **103 Suppl 1,** 135-142.

Moore-Hoon M. L. and Turner R. J. (2000) The structural unit of the secretory Na+-K+-2Cl-cotransporter (NKCC1) is a homodimer. *Biochemistry* **39,** 3718-3724.

Mosmann T. (1983) Rapid colorimetric assay for cellular growth and survival: application to proliferation and cytotoxicity assays. *J. Immunol. Methods* **65,** 55-63.

Nini L., Waheed A. A., Panicker L. M., Czapiga M., Zhang J. H. and Simonds W. F. (2007) R7-binding protein targets the G protein beta 5/R7-regulator of G protein signaling complex to lipid rafts in neuronal cells and brain. *BMC. Biochem.* **8,** 18.

Nothwang H. G., Becker M., Ociepka K. and Friauf E. (2003) Protein analysis in the rat auditory brainstem by two-dimensional gel electrophoresis and mass spectrometry. *Mol. Brain Res.* **116,** 59-69.

O'Connell K. M. and Tamkun M. M. (2005) Targeting of voltage-gated potassium channel isoforms to distinct cell surface microdomains. *J. Cell Sci.* **118,** 2155-2166.

Pike L. J. (2004) Lipid rafts: heterogeneity on the high seas. *Biochem. J.* **378,** 281-292.

Pike L. J. (2006) Rafts defined: a report on the Keystone Symposium on Lipid Rafts and Cell Function. *J. Lipid Res.* **47,** 1597-1598.

Plotkin M. D., Snyder E. Y., Hebert S. C. and Delpire E. (1997) Expression of the Na-K-2Cl Cotransporter is Developmentally Regulated in Postnatal Rat Brains: A Possible Mechanism Underlying GABA's Excitatory Role in Immature Brain. *J Neurobiol* **33,** 781-795.

Price G. D. and Trussell L. O. (2006) Estimate of the chloride concentration in a central glutamatergic terminal: a gramicidin perforated-patch study on the calyx of Held. *J. Neurosci.* **26,** 11432-11436.

Rivera C., Voipio J., Payne J. A., Ruusuvuori E., Lahtinen H., Lamsa K., Pirvola U., Saarma M. and Kaila K. (1999) The K+/Cl- co-transporter KCC2 renders GABA hyperpolarizing during neuronal maturation. *Nature* **397,** 251-255.

Rodgers W. and Rose J. K. (1996) Exclusion of CD45 inhibits activity of p56lck associated with glycolipid-enriched membrane domains. *J. Cell Biol.* **135,** 1515-1523.

Russell J. M. (2000) Sodium-potassium-chloride cotransport. *Physiol. Rev.* **80,** 211-276.

Scandroglio F., Venkata J. K., Loberto N., Prioni S., Schuchman E. H., Chigorno V., Prinetti A. and Sonnino S. (2008) Lipid content of brain, brain membrane lipid domains, and neurons from acid sphingomyelinase deficient mice. *J. Neurochem.* **107,** 329-338.

Scheek S., Brown M. S. and Goldstein J. L. (1997) Sphingomyelin depletion in cultured cells blocks proteolysis of sterol regulatory element binding proteins at site 1. *Proc. Natl. Acad. Sci. U. S. A* **94,** 11179-11183.

Schuck S., Honsho M., Ekroos K., Shevchenko A. and Simons K. (2003) Resistance of cell membranes to different detergents. *Proc. Natl. Acad. Sci. U. S. A* **100,** 5795-5800.

Simard C. F., Daigle N. D., Bergeron M. J., Brunet G. M., Caron L., Noel M., Montminy V. and Isenring P. (2004) Characterization of a novel interaction between the secretory Na+-K+-Cl-cotransporter and the chaperone hsp90. *J. Biol. Chem.* **279,** 48449-48456.

Sipila S. T., Huttu K., Yamada J., Afzalov R., Voipio J., Blaesse P. and Kaila K. (2009) Compensatory enhancement of intrinsic spiking upon NKCC1 disruption in neonatal hippocampus. *J. Neurosci.* **29,** 6982-6988.

Song L. Y., Mercado A., Vazquez N., Xie Q. Z., Desai R., George A. L., Gamba G. and Mount D. B. (2002) Molecular, functional, and genomic characterization of human KCC2, the neuronal K-Cl cotransporter. *Mol. Brain Res.* **103,** 91-105.

Strange K., Singer T. D., Morrison R. and Delpire E. (2000) Dependence of KCC2 K-Cl cotransporter activity on a conserved carboxy terminus tyrosine residue. *American Journal of Physiology - Cell Physiology* **279,** C860-C867.

Taverna E., Saba E., Rowe J., Francolini M., Clementi F. and Rosa P. (2004) Role of lipid microdomains in P/Q-type calcium channel (Cav2.1) clustering and function in presynaptic membranes. *J. Biol. Chem.* **279,** 5127-5134.

Vardi N., Zhang L. L., Payne J. A. and Sterling P. (2000) Evidence that different cation chloride cotransporters in retinal neurons allow opposite responses to GABA. *J. Neurosci.* **20,** 7657-7663.

Welker P., Bohlick A., Mutig K., Salanova M., Kahl T., Schluter H., Blottner D., Ponce-Coria J., Gamba G. and Bachmann S. (2008) Renal Na+-K+-Cl- cotransporter activity and vasopressin-induced trafficking are lipid raft-dependent. *Am. J. Physiol Renal Physiol* **295,** F789-F802.

Wenz M., Hartmann A. M., Friauf E. and Nothwang H. G. (2009) CIP1 is an activator of the K+-Cl- cotransporter KCC2. *Biochem. Biophys. Res. Commun.* **381,** 388-392.

Williams J. R. and Payne J. A. (2004) Cation transport by the neuronal K(+)-Cl(-) cotransporter KCC2: thermodynamics and kinetics of alternate transport modes. *Am. J. Physiol Cell Physiol* **287,** C919-C931.

Yamada J., Okabe A., Toyoda H., Kilb W., Luhmann H. J. and Fukuda A. (2004) Cl- uptake promoting depolarizing GABA actions in immature rat neocortical neurones is mediated by NKCC1. *J. Physiol* **557,** 829-841.

Yu C., Alterman M. and Dobrowsky R. T. (2005) Ceramide displaces cholesterol from lipid rafts and decreases the association of the cholesterol binding protein caveolin-1. *J. Lipid Res.* **46,** 1678-1691.

Zhu L., Lovinger D. and Delpire E. (2005) Cortical neurons lacking KCC2 expression show impaired regulation of intracellular chloride. *J. Neurophysiol.* **93,** 1557-1568.

FIGURE CAPTIONS

Fig. 1 Different solubility of NKCC1 and KCC2 in Brij 58. Membranes were prepared from 1.5 mg brain tissue of P25-30 rats, solubilized in 1% Brij 58 with a protein to detergent ratio of 1 : 2.5 for 30 min, and subjected to flotation experiments through a discontinuous sucrose gradient. Twelve fractions were collected, and their protein content was separated by SDS-PAGE. Immunoblots were probed for the abundance of NKCC1, KCC2, Na^+/K^+-ATPase, flotillin-1, and transferrin receptor (TfR). (A) NKCC1 was enriched in the low density, Brij 58-insoluble fractions 4-6, codistributing with flotillin-1. For KCC2, a detergent-insoluble and a detergent-soluble KCC2 pool became apparent. The alpha subunit of the Na^+/K^+-ATPase was largely solubilized and appeared in the high-density fractions. (B) Removal of cholesterol from the membrane homogenate by methyl-ß-cyclodextrin (MßCD) prior to extraction with Brij 58 resulted in a shift of KCC2 towards higher-density fractions, whereas NKCC1 was still recovered in low density fractions. The Na^+/K^+-ATPase was exclusively present in the high-density fractions. Monitoring of cholesterol content was performed using a cholesterol assay kit. Note that the black triangle on top solely indicates the increase of sucrose density towards the bottom of the centrifuge tube, without implying a linear rise. Blots shown are representatives of four (A) or two (B) experiments.

Fig. 2 Detergent-soluble and detergent-insoluble cotransporters display complex glycosylation patterns in the mature brainstem. Gradient fractions from membranes of the mature brain enriched in either Brij 58-soluble or Brij 58-insoluble KCC2 were pooled and treated with the endoglycosidase EndoH (A) or the amidase PGNase F (B). After separation in a linear 4-12% Bis-Tris NuPAGE system, immunoblot analysis was performed for KCC2. In both the detergent-soluble and the detergent-insoluble pools, the cotransporters were EndoH insensitive, as no shift in molecular weight was observed compared to the untreated samples. In contrast, PGNase treatment induced a shift towards lower molecular weights. Each blot shows an example of two independent experiments with similar results.
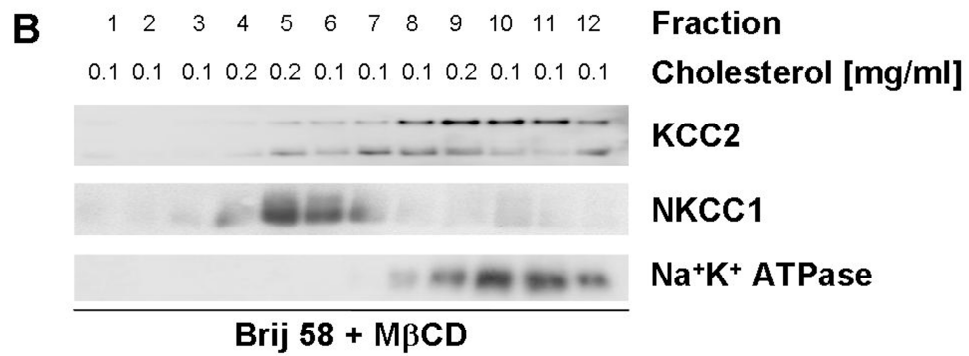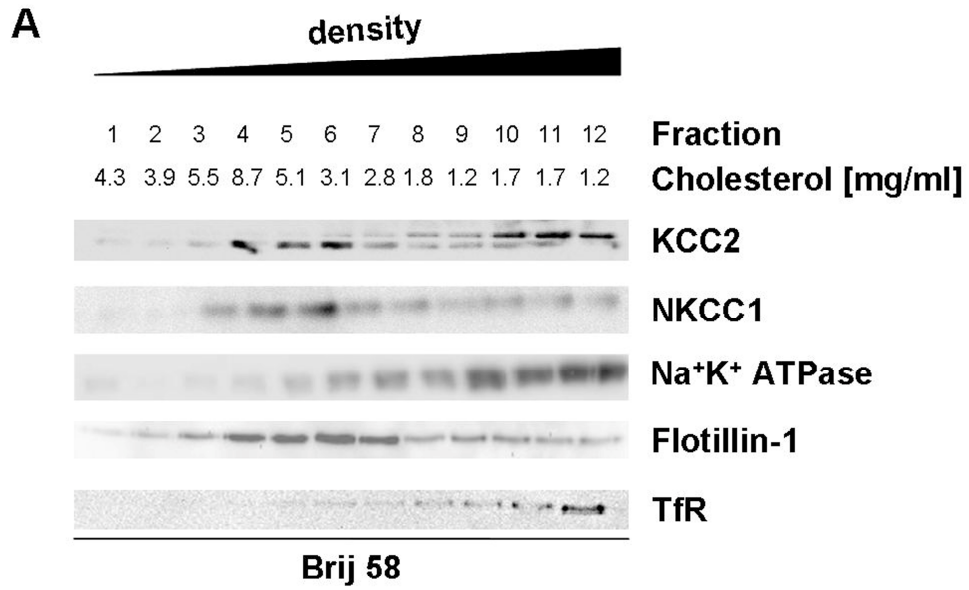
Fig. 3 Disruption of membrane rafts differentially affects NKCC1 and KCC2 transport activity. HEK-293 cells were incubated with MβCD, with SMase, or a combination of both agents and then assayed for $^{86}Rb^+$ uptake. (A) KCC2 expressing cells showed a more than 3-fold increased $^{86}Rb^+$ uptake after cholesterol depletion by MβCD ($300.1 \pm 45.7\%$; $p = 8.4 \times 10^{-19}$) and a 6.7-fold increase after combined action of both agents ($671.7 \pm 152.4\%$; $p = 6.9 \times 10^{-20}$). MßCD
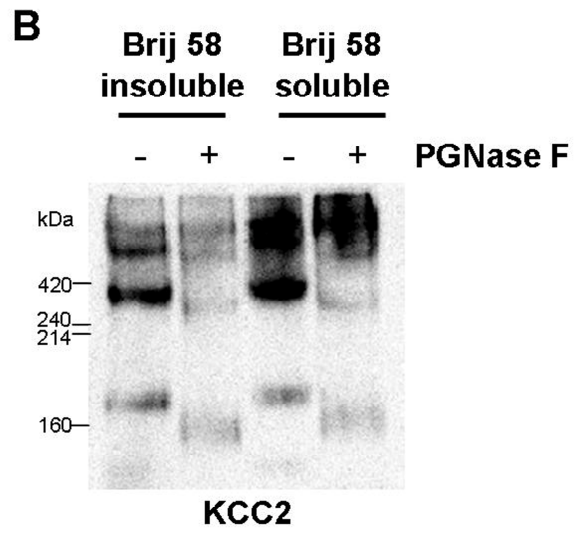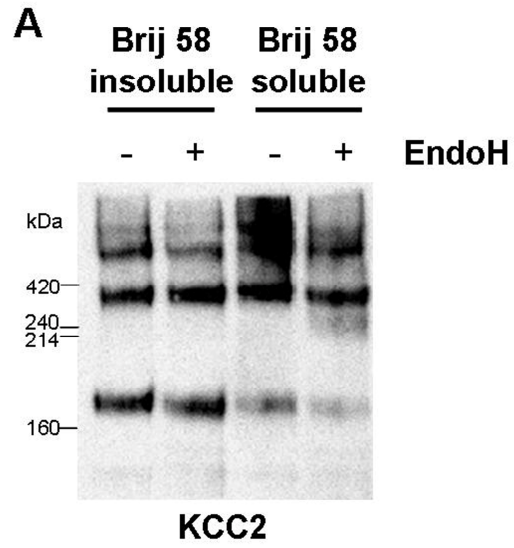
treatment increased KCC2 activity slightly ($142.9 \pm 15.1\%$; $p = 6.1 \times 10^{-12}$). 2 mM furosemide blocked most of the increased flux. 100% flux corresponded to 14.4 ± 2.4 nmoles $\times$ mg protein^{-1} $\times$ min^{-1}. (B) Native HEK-293 cells expressing NKCC1 showed a 1.7-fold reduced ^{86}Rb^{+} uptake after SMase treatment ($58.3 \pm 9.6\%$; $p = 1.3 \times 10^{-7}$) and a 4-fold decrease after combined action of both agents ($38.6 \pm 17.1\%$; $p = 2 \times 10^{-9}$). MßCD had only a minor effect ($144 \pm 19.1\%$, $p = 1.1 \times 10^{-6}$). The flux in native cells under normal condition and after MßCD treatment was completely blocked by 10 µM bumetanide. Flux data were corrected for changes in cell viability The plot shows the mean $\pm$ s.d. $n \geq 6$.
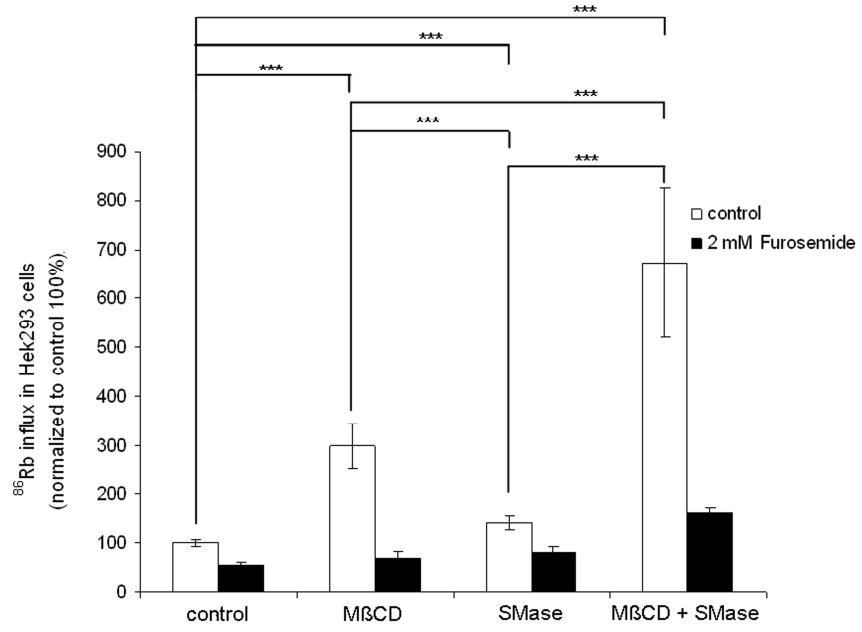
Fig. 4 Disruption of membrane rafts alters cluster size of KCC2 and NKCC1 at the plasma membrane. EGFP-tagged KCC2- and NKCC1-expressing HEK-293 cells (A-H and I-P, respectively) were treated with MβCD (B, F, J, N), SMase (C, G, K, O), or a combination of both agents (D, H, L, P). After incubation, cells were processed for confocal imaging. The distribution of the tagged transporters is shown in cross-sections (A-D, I-L) and at the basal surface of the respective cells (E-H, M-P). Treatment with MβCD or SMase alone did not cause major changes in the distribution of the transporters. After the combined treatment, however, the transporters became located in large clusters at the plasma membrane (H, P), visible as bright spots in the membrane region in cross-sections (arrows in D and L). Bar 10 µm.

Fig. 5 Membrane raft association of KCC2 in the immature brainstem. Membranes were prepared from 1.5 mg brainstem tissue of P0-2 rats, solubilized in 1% Brij 58 for 30 min, and subjected to flotation experiments through a discontinuous sucrose gradient. Twelve fractions were collected, and their protein content was separated by 10% SDS-PAGE. Immunoblots were probed for the abundance of KCC2, flotillin-1, and TfR. KCC2 was insoluble in Brij 58, codistributing with flotillin-1 in the low density fractions. Cholesterol depletion by MβCD resulted in efficient extraction of KCC2 by Brij 58. The blots are representative examples of two to three independent experiments.

Suppl. Figure 1 Cell viability and cholesterol depletion in HEK-293 cells. (A) Treatment of HEK-293 cells with 10 mg/ml MβCD for 30 min depleted 45% of the membrane cholesterol content. The plot shows the mean $\pm$ s.d., $n \geq 6$. (B) HEK-293 cells were treated with 10 mg/ml MβCD to deplete cholesterol, with 100 mU/ml SMase to break down sphingomyelin, or with a combination of both agents, and cell viability was determined by an MTT assay. Viability was ~90% after treatment with either of the two agents and 74% after combined action.

A

density

1	2	3	4	5	6	7	8	9	10	11	12	Fraction
4.3	3.9	5.5	8.7	5.1	3.1	2.8	1.8	1.2	1.7	1.7	1.2	Cholesterol [mg/ml]

KCC2

NKCC1

Na$^+$K$^+$ ATPase

Flotillin-1

TfR

Brij 58

B

1	2	3	4	5	6	7	8	9	10	11	12	Fraction
0.1	0.1	0.1	0.2	0.2	0.1	0.1	0.1	0.2	0.1	0.1	0.1	Cholesterol [mg/ml]

KCC2

NKCC1

Na$^+$K$^+$ ATPase

Brij 58 + MβCD

A

Brij 58 insoluble   Brij 58 soluble

−   +   −   +   **EndoH**

kDa

420—

240—
214—

160—

KCC2

B

Brij 58 insoluble   Brij 58 soluble

−   +   −   +   **PGNase F**

kDa

420—

240—
214—

160—

KCC2

A

B

| | control | MßCD | SMase | SMase/MßCD |

density

A   1 2 3 4 5 6 7 8 9 10 11 12   Fraction

KCC2

Flotillin-1

TfR

Brij 58

B   1 2 3 4 5 6 7 8 9 10 11 12

KCC2

Brij 58 + MβCD